*Poster contributions of the "Advanced Lectures on the Starburst-AGN Connection", Eds. R. Mújica, I. Aretxaga & D. Kunth, 2001, INAOE Electronic Edition (http://www.inaoep.mx/∼agn00/posters.html), pp. 93-96*

# Do Massive Dark Cores Exist in Spiral Galaxies?

**T. Takamiya and Y. Sofue**

Institute of Astronomy, Univ. of Tokyo, Mitaka, Tokyo 181-0015, Japan

**Abstract.** We explore the inner-most region of nearby spiral galaxies. First, exact rotation curves of them are to be obtained. From position-velocity diagrams, the observational data, we derive rotation curves, the reduced data, by carrying out the iterative fitting calculations. Next, after checking the accuracy of the rotation-curve data, we derive radial profiles of the surface-mass density directly from them. Finally, with the corresponding luminosity profiles, the radial distribution of the mass-to-luminodity ratios ($M/L$) from the inner bulge ($\sim$ a few 100 pc) to the outer disk (more than 2 to 10 kpc) for 11 galaxies are obtained. The $M/L$s in the bulges of some galaxies with sufficiently high spatial resolutions are found to increase steeply toward the center at radii $\sim$ 100 to 500 pc. Other galaxies with high resolutions also appear to show signs of an increase. We result in the three possibilities: (1) Dark matter, same as that in a massive dark halo, is also dominant around the nucleus. (2) In some galaxies, there are active star forming regions concerning the inner Lindblad resonances (ILRs). (3) We cannot completely ignore the effect of gas-extinction in the inner-most region, though this influence seems to be not serious with near-IR photometry data. (1) might indicate a new component, a 'massive dark core', which is an object linking a bulge and a central black hole.

## 1. Introduction

The mass distribution of the inner part of an extragalaxy is essential for the activity and the history of the galactic formation. In the case of spiral galaxies, 1-dimensional surface-mass density (hereafter SMD) can be calculated from a rotation curve (RC). RCs in disk and outer regions have been derived from position-velocity (PV) diagrams obtained by optical and HI-line spectroscopy (Rubin et al. 1980, 1982, 1985; Bosma 1981a; Mathewson et al. 1992; Persic & Salucci 1995; Mathewson & Ford 1996; Clemens 1995; Sofue 1996, 1997; Honma & Sofue 1997). Recently, we have obtained inner-most RCs by analyzing high-resolution CO, H$\alpha$, and [NII]-line spectroscopic data (Sofue 1996, 1997; Sofue et al. 1997, 1998, 1999). The most popular and straightforward way of the derivation is to trace peak-flux points of PV diagrams. But this method fails to measure the correct velocity in the circumnuclear region where the velocity gradient is large. It depends on the beam size, including the slit width and an inclination of a galaxy, and the gas deficiency. As a result of our recent observations (Sofue et al. 1999) many of Sb & Sc galaxies have steeply rising rotation curves in the central regions, with which we must be careful.

Radial profiles of the surface-mass density (SMD) and the surface luminosity can be used to calculate the mass-to-luminosity ($M/L$) ratio directly. A Radial variation of the $M/L$ ratio in a galaxy is a clue to investigate the distributions of visible and dark (invisible) masses (e.g., Kent 1986, 1987; Persic & Salucci 1988, 1990; Salucci & Frenk 1989; Forbes 1992; Persic et al. 1996; Héraudeau & Simien 1997; Rubin et al. 1997). However, most of the current studies have been devoted to investigate the dark halo, which is supposed to be closely related to galaxy formation and the stability of disks (e.g., Ostriker & Peebles 1973; Athanassoula et al. 1987). On the other hand, there have been few systematic investigations of dark matter within a bulge and an inner disk, for which, however, high-resolution and high-quality rotation curves are required as well as corresponding luminosity profiles. Here,we evaluate the accuracy of RCs by the iterative calculations in the next section, and derive SMD and $M/L$ profiles in section 3, and discuss the results in section 4.

## 2. Deriving Exact Rotation Curves

Generally, an RC has been derived by tracing peak-flux positions of the PV diagram. But in the inner-most region where an RC is steeply rising outwards, it does not correspond with a peak-flux profile because of various observational parameters (seeing, a slit width, an inclination of a galaxy and a spectral resolution) and the distribution of gas. For example, if a spatial resolution and slit width are quite large, we observe much more gas with line-of-sight velocity equal to zero near the center, whether the real rotation velocity there is high or not.

To derive exact RCs, we invent the "iterative fitting method". This method is following:

(1) We define the peak-flux velocity profile of the PV diagram as the initial RC, V0($r$). We also define the temporary RC, V1($r$), first set to equal to the V0($r$).

(2) We assume that V1($r$) is the real RC, and calculate the PV diagram besed on the RC and the real observational parameters.

(3) We again derive the RC from the peak-flux velocity profile of the simulated PV diagram, and define it as V2($r$).

(4) We calculate the Vgap($r$) = V0($r$) − V2($r$), and if the Vgap($r$) is less than 10 km/s in the whole region, we succesfully finish the fitting. But if not so, we add the −Vgap($r$) to the V1($r$), re-define it as V1($r$) and go back to the step (2). This iteration is continued until the convergence is attained.

We first apply this method to some model RCs, and confirm that the convergence is attained in most cases. The estimated error is about 10 km/s, corresponding to the convergent condition. Next, we apply it to the observational data, including noise and a complicated gas distribution. We use the data obtained from the optical spectroscopic observation by the Okayama 188 cm telescope in March 1997 (Sofue et al. 1998) and March 1999. We succeed in the convergence for some data with high signal-to-noise ratios. We show the result for Sbc galaxy NGC 5055 in Fig. 1 and 2. In Fig. 3 the difference between the RC after the iteration and the initial RC, V0($r$) is shown. It is obvious that we are easy to underestimate the velocity in the inner-most region systematically.

In the following we use the RC data in Sofue (1997), where RCs are derived by the "envelope-tracing method". This method is also to correct the underestimation of velocity in the central region. To verify the validity and the accuracy of this method, we carry out this method and the iterative fitting method for some observational data. It is noted that the peak velocities at $r \sim$ (spatial resolution) nearly coincide between the two methods, while that of the peak-flux velocity profile is less than them by 50 km/s at most. The profiles by the two methods are largely different near the center, $r \sim 1-2''$, but this is caused by limited spatial resolutions. We conclude that the error of velocity by the envelope-tracing method is 15 - 20 km/s.

## 3. SMD and $M/L$ profiles

We assume that the 'true' SMD in a real disk galaxy will be between two extreme cases; spherical and axisymmetric flat-disk distributions. We can calculate the SMD, $\sigma(R)$, directly from an RC for these extreme cases. This estimation is independent of model components of a galaxy and can indicate the radial variance of the total mass, including dark matter.

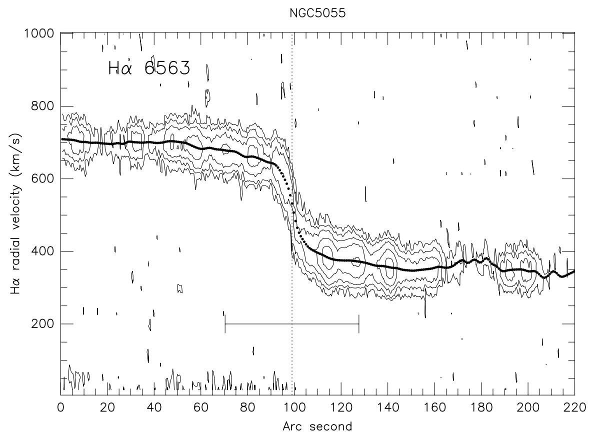


**Fig. 1.** The PV diagram (Hα line) & the peak-flux velocity profile of NGC 5055 (horizontal bar=2kpc)

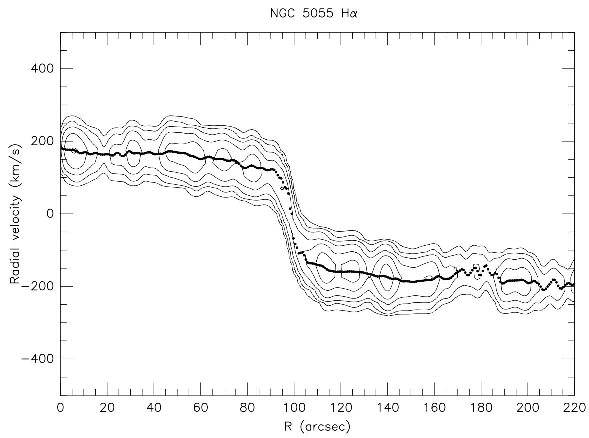


**Fig. 2.** The calculated PV-diagram and the rotation curve after the iterative fitting method

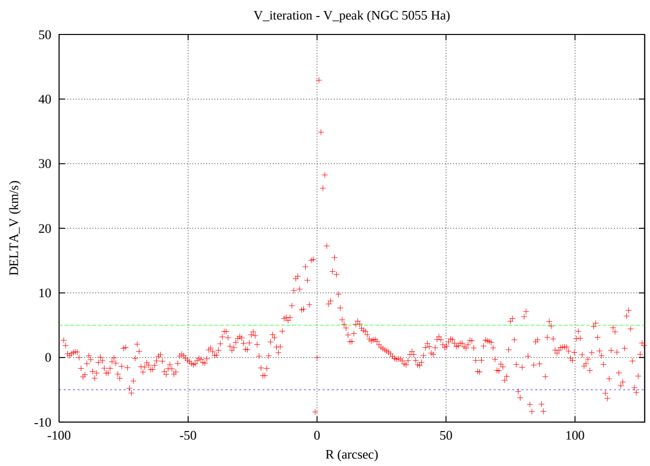


**Fig. 3.** The difference between the peak-flux velocity and the velocity derived from the iterative fitting method.

The SMD under the spherical distribution $\sigma_S(R)$ is calculated by,

$$\sigma_S(R) = \frac{1}{2\pi} \int_R^\infty \frac{1}{r\sqrt{r^2 - R^2}} \frac{dM(r)}{dr} dr, \quad (1)$$

where the mass $M(r)$ inside the radius $r$ is given by $M(r) = rV(r)^2 G^{-1}$. The SMD for a thin flat-disk, $\sigma_D(R)$, is derived by solving the Poisson's equation:

$$\sigma_D(R) = \frac{1}{\pi^2 G}\left[\frac{1}{R}\int_0^R \left(\frac{dV^2}{dr}\right)_x K\left(\frac{x}{R}\right) dx + \int_R^\infty \left(\frac{dV^2}{dr}\right)_x K\left(\frac{R}{x}\right)\frac{dx}{x}\right], \quad (2)$$

where $K$ is the complete elliptic integral (Binney & Tremaine 1987).

We use the RCs in Sofue (1997) to derive the SMD profiles. We select 18 SA and SAB spiral galaxies, for which the spatial resolution (FWHM) is less than 650 pc. The typical difference of SMD values between the two assumptions (sphere and flat-disk) is estimated to be $\pm 0.05$ to 0.1 in a logarithmic scale. The error due to the error in rotation velocities is about $\pm 0.05$. Hence, the effective error of SMD calculation is estimated to be $\pm 0.1$ to 0.15. Although some Sc galaxies distinctly have smaller SMD values than the average, the difference in SMD between the two galaxy types is small. In the inner bulge region, SMDs show the isothermal-sphere increases. Though the present sample includes galaxies showing Seyfert (NGC 1068, NGC 4569), LINER (NGC 3521, NGC 4569), jets (NGC 3079), and black holes (the Milky Way), the central activities appear to be not directly correlated with the mass distribution.

Dividing an SMD by the corresponding luminosity profile, we obtained the $M/L$ profiles for 11 galaxies. Fig. 4 shows the result of NGC 4527, an SABbc galaxy. The angular resolution of this RC data is $2''$, corresponding to 210 pc if D = 22 kpc.

## 4. Results

We summarize the general characteristics of the $M/L$ behavior as follows:
(1) The $M/L$ remains nearly constant in the inner disk.
(2) It increases gradually outward in the outer disk for all the galaxies.
(3) The $M/L$ increases more steeply in the outer halo, indicating the massive dark halo.
(4) Bulge components show a constant or a slightly smaller value than the disk value.
(5) For some galaxies with high spatial resolution, the $M/L$ increases steeply toward the nucleus inside the bulge.

The results of (4) and (5) have not been pointed out, because a spiral galaxy has been assumed to consist of

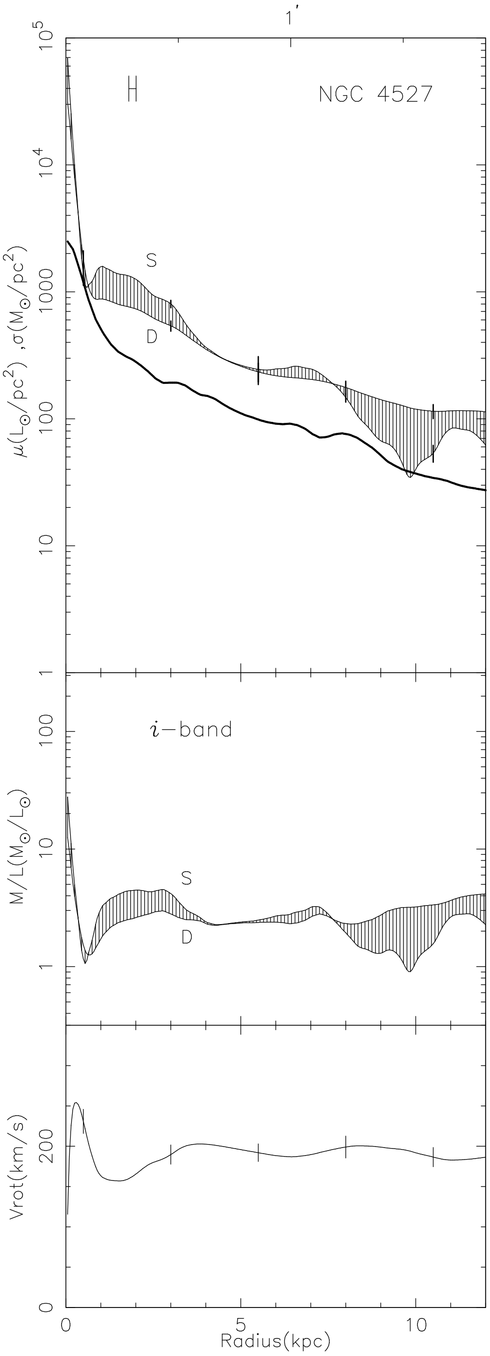


**Fig. 4.** Top: (S) Surface-mass-density profile of NGC 4527 for the spherical assumption. (D) Same but for the flat-disk assumption. An bold line denotes the luminosity profile, corrected for the inclination. Middle: Mass-to-Luminosity ratio for (S) spherical and (D) flat-disk assumptions. Bottom: Rotation curve. The error-bars are caused mainly by those of rotation curve. The true values of the surface-mass-density will lie in the shaded area between (S) and (D). The horizontal error-bar in the top-left corner denotes the angular (spatial) resolution of the surface-mass-density (FWHM), which is larger than that of the luminosity profile in all the cases. The interval of the shading lines corresponds to a double of the interval of data sampling points.

three or four components only; a central black hole, a spheroidal bulge, a flat disk, and a dark halo. In a bulge and a disk, each statistical characteristic of stars has been assumed to be invariable to the distance from the center, so this new component is, even if any, overlooked.

In the results of (4) and (5), we expect three possibilities:

(a) Dark matter, same as that in a massive dark halo, may be also dominant around the galactic nucleus. It implies that the bulges contain an excess of (dark) mass inside a few hundred pc, which we call a "massive dark core" with a scale radius of 100 - 200 pc.

(b) The compostion of stars may be varying in bulge region. In active star forming region, many massive young stars cause low mass-to-luminosity ratio. So if the activity is quite low in the inner-most region, it looks like dark core around the nucleus.

(c) We may not be able to ignore the influence of extinction by gas in the inner-most region. The influence is more serious in using optical luminosity data than near-IR data.

As the spatial resolutions of the data range from 100 pc to 650 pc, we should be careful to discuss increasing $M/L$ among the galaxies. But it is interesting to discuss the radial variance of a individual galaxy. Especially, the drastic increase of $M/L$ within $r = 500$ pc for NGC 4527 is of particular interest; the increase amounts to $4.9 \pm 1.0$ times/350pc from $r = 500$ to 150 pc. Since the results are based on optical data, these values may be overestimated because of optical extinction. However, it is known that color gradients like $V - K$ and $r - K$ of face-on galaxies are of the order of 1 mag arcsec$^{-2}$ (e.g., de Jong & van der Kruit 1994; Terndrup et al. 1994). For NGC 4527 with $i = 60° - 75°$, the $B - K^{'}$ color gradient is estimated to be about 1.5 mag arcsec$^{-2}$ (Héraudeau et al. 1996). In the present data, the luminosity profile of NGC 4527 is in the Thuan-Gunn $i$-band, and we may conclude that the central increase of $M/L$ for NGC 4527 will be also significant.

It is also interesting to apply the case (a). If the rotational velocity at $r = 200$ pc is 200 km s$^{-1}$, $M \sim RV^2/G = 1.8 \times 10^9 M_{\odot}$. This core component could be an object linking the galactic bulge with a massive black hole in the nuclei (Miyoshi et al. 1995; Genzel et al. 1997; Ghez et al. 1998) and/or massive core objects causing a central Keplerian RC (Bertola et al. 1998).

## References


Athanassoula, A., Bosma, A., & Papaioannou, S. 1987, A&AS, 179, 23

Bertola, F., Cappellari, M., Funes, J.G., Corsini, E.M., Pizzella, A., & Vega-Bertran, J.C. 1998, ApJ, 509, L93.

Binney, J., & Tremaine, S. 1987, Galactic Dynamics (Princeton Univ. Press)

Bosma, A. 1981, AJ, 86, 1791

Clemens, D.P. 1985, ApJ, 295, 42

de Jong, R.S., & van der Kruit, P.C. 1994, A&AS, 106, 451

Forbes, D.A. 1992, A&AS, 92, 583

Genzel, R., Eckart, A., Ott, T., & Eisenhauer, F. 1997, MNRAS, 291, 219

Ghez, A.M., Klein, B.L., Morris, M., & Becklin, E.E. 1998, ApJ, 509, 678.

Héraudeau, Ph., Simien, F., & Mamon, G.A. 1996, A&AS, 117, 417

Héraudeau, Ph., & Simien, F. 1997, A&A, 326, 897

Honma, M., & Sofue, Y. 1997, PASJ, 49, 453

Honma, M., & Sofue, Y. 1997, PASJ, 49, 539

Kent, S.M. 1986, AJ, 91, 1301

Kent, S.M. 1987, AJ, 93, 816

Mathewson, D.S., Ford, V.L., & Buchhorn, M. 1992, ApJS, 81, 413

Mathewson, D.S., & Ford, V.L. 1996, ApJS, 107, 97

Miyoshi, M., Moran, J., Herrnstein, J., Greenhill, L., Nakai, N., Diamond, P., & Inoue, M. 1995, Nature, 373, 127.

Ostriker, J.P., & Peebles, P.J.E. 1973, ApJ, 186, 467

Persic, M., & Salucci, P. 1988, MNRAS, 234, 131

Persic, M., & Salucci, P. 1990, MNRAS, 245, 577

Persic, M., & Salucci, P. 1995, ApJS, 99, 501

Persic, M., Salucci, P., & Stel, F. 1996, MNRAS, 281, 27

Rubin, V.C., Ford, W.K., & Thonnard, N. 1980, ApJ, 238, 471

Rubin, V.C., Ford, W.K., & Thonnard, N. 1982, ApJ, 261, 439

Rubin, V.C., Burstein, D., Ford, W.K.,JR., & Thonnard, N. 1985, ApJ, 289, 81

Rubin, V.C., Kenny, J.D.P., & Young, J.S. 1997, AJ, 113, 1250

Salucci, P., & Frenk, C.S. 1989, MNRAS, 237, 247

Sofue, Y. 1996, ApJ, 458, 120

Sofue, Y. 1997, PASJ, 49, 17

Sofue, Y., Tutui, Y., Honma, M., & Tomita, A. 1997, AJ, 114, 2428

Sofue, Y., Tomita, A., Honma, M., Tutui, Y., & Takeda, Y. 1998, PASJ, 50, 427

Sofue, Y., Tutui, Y., Honma, M., Tomita, A., Takamiya, T., Koda, J., & Takeda, Y. 1999, ApJ, 523, 136

Takamiya, T., & Sofue, Y. 2000a, ApJ, 534, 670

Takamiya, T., & Sofue, Y. 2000b, in preparation

Terndrup, D.M., Davies, R.L., Frogel, J.A., DePoy, D.L., & Wells, L.A. 1994, ApJ, 432, 518